Homologous Association of Oppositely Imprinted Chromosomal Domains

Janine M. LaSalle and Marc Lalande*

Human chromosome 15q11-q13 encompasses the Prader-Willi syndrome (PWS) and the Angelman syndrome (AS) loci, which are subject to parental imprinting, a process that marks the parental origin of certain chromosomal subregions. A temporal and spatial association between maternal and paternal chromosomes 15 was observed in human T lymphocytes by three-dimensional fluorescence in situ hybridization. This association occurred specifically at the imprinted 15q11-q13 regions only during the late S phase of the cell cycle. Cells from PWS and AS patients were deficient in association, which suggests that normal imprinting involves mutual recognition and preferential association of maternal and paternal chromosomes 15.

Parental imprinting is an epigenetic process that distinguishes the parental origin of certain chromosomal subregions in higher eukaryotes, resulting in allele-specific differences in methylation, transcription, and replication (*1–3*). In humans, imprinting is evident from the phenotypically distinct genetic disorders PWS and AS, which result from the lack of a paternal or maternal contribution to the chromosome 15q11-13 region, respectively (*4*). One manifestation of imprinting is allele-specific replication. For most loci examined in the PWS-AS region, paternal alleles replicate earlier than maternal alleles (*3, 5*). There is, however, a small region between the γ-aminobutyric acid receptor β3 (GABRB3) and α5 (GABRA5) subunit genes, where the opposite pattern of allele-specific replication timing is observed (6). This organization of replication timing domains is perturbed in cells of individuals with PWS and AS, which suggests that association and transregulation between the maternal and paternal chromosomes is required for the normal pattern of imprinting in chromosome 15q11-q13. Trans interactions between homologous chromosomes are important for normal development in *Drosophila*, where it has been shown that transvection depends on homologous pairing (*7*). Homologous pairing has been defined as the preferential association of homologous chromosomes in meiotic and somatic eukaryotic cells (8).

The possibility of association between homologous chromosomes 15 was directly examined here by confocal laser scanning microscopy and three-dimensional fluorescence in situ hybridization (3D FISH) with the use of a chromosome 15 centromeric probe (D15Z1) and a control chromosome 12 centromeric probe (D12Z3) (Fig. 1A). Nuclei were optically sectioned and distances were measured between the *x*, *y*, and *z* coordinates at the center of each hybridization signal (9). The distances measured between heterologous D15Z1 and D12Z3 signals are randomly distributed in a linear swarm between 0.2 μm to 12 μm in normal cycling lymphocytes. The distances between homologous D12Z3 signals fell within the random distribution, but D15Z1 interhomolog distances were slightly less than expected for a random distribution (*10*). This small difference in chromosome 15 homologous distances relative to those between other centromeres has been observed previously and ascribed to the role of the chromosome 15p arms in organizing the nucleolus (*11*). As temporal and spatial repositioning of chromosomes occurs during the cell cycle (*12*), an additional possibility is that homologous association is a transient event that may be difficult to detect in the total cell population.

Fluorescence-activated cell sorting was therefore used to fractionate lymphocytes into four stages of the cell cycle before 3D FISH. Heterologous distances in each cell cycle stage fell within a linear swarm expected for a random distribution from minimum (0.2 μm pixel resolution) to maximum nuclear diameter (*13*) (Fig. 1B). These results demonstrate that chromosome 15 centomeric signals are closer together than expected from random in the late S phase, but not in other cell cycle stages. In contrast, distances between chromosome 12 centromeric signals are randomly distributed in all cell cycle stages. A distance of ≤2.0 μm was selected to define a close association between two signals (*14*). In the late S phase, 16 nuclei (32%) had interhomolog distances ≤2.0 μm at D15Z1 loci, whereas only 2% of nuclei had interhomolog distances within this range at D12Z3.

To determine if the transient association of D15Z1 signals was simply a result of the participation of 15p arms in nucleolar organization or the result of a more specific interaction, we also analyzed genomic probes from 15q by 3D FISH (*15*) (Fig. 2). A specific probe from the proximal long arm (D13S104, q12-q13) of chromosome 13 was used as a control for another chromosome involved in nucleolar organization and was hybridized together with GABRB3/A5 from 15q11-13. The average heterologous distances between the chromosome 13 and 15 probes were less than those between D15Z1 and D12Z3 (compare the slopes determined by the plus signs in Figs. 1B and 2B). In the late S phase, however, 58% of the nuclei exhibited GABRB3/A5 interhomolog distances ≤2.0 μm. In contrast, only 22% of the nuclei exhibited the same close association of D13S104 homologs. These results suggest that there is a specific association of chromosome 15 homologs in addition to their acrocentric effect on nucleolar organization.

The marked increase in the number of nuclei with closely associated 15q11-13 loci (GABRB3/A5, Fig. 2B) relative to the centromeric region (D15Z1, Fig. 1B) suggests

Table 1. Determination of the closest region of association by comparison of interhomolog distances of different chromosome 15 loci. Probe order (and band localization) from centromeric proximal to distal is as follows: D15Z1-D15S128 (q11-13)-D15S113 (q11-13)-GABRB3/A5 (q11-13)-D15S46 (q25-26). For these analyses, measurements were directly compared on a per nucleus basis to avoid minor differences in nuclei size and shape between sample sets in different experiments. For each data set of 50 late S phase nuclei, we selected nuclei in which either homologous distance was ≤2.0 μm. Interhomolog distances of both probes within each nucleus were compared. The numbers of nuclei with the green interhomolog distance less than the red interhomolog distance and vice versa are indicated.

Probe combination		Nuclei with interhomolog distances ≤2.0 μm		Conclusion
Green	Red	Green ≤ red	Red ≤ green	
GABRB3/A5	D15Z1	20*	6	GABRB3/A5 < D15Z1
GABRB3/A5	D15S46	25*	5	GABRB3/A5 < D15S46
D15S128	GABRB3/A5	17	18	D15S128 = GABRB3/A5
GABRB3/A5	D15S113	10	13	GABRB3/A5 = D15S113
D15S113	D15S46	24*	6	D15S113 < D15S46
D15S128	D15Z1	17*	1	D15S128 < D15Z1
D15S46	D15Z1	7	17*	D15Z1 < D15S46

*Values are statistically significant as determined by a χ^2 test.

Howard Hughes Medical Institute, Genetics Division, Children's Hospital, and Department of Pediatrics, Harvard Medical School, Boston, MA 02115, USA.

*To whom correspondence should be addressed.

that the closest interaction between homologs involves the imprinted region of chromosome 15. To determine if the imprinted region was closer than the nonimprinted region, we performed dual hybridizations with several chromosome 15 probe combinations, including centromeric D15Z1, three probes from q11-13, and a control probe from the nonimprinted telomeric end of chromosome 15 (Table 1). The imprinted 15q11-13 region was closer than both the centromere and the nonimprinted control, but the three loci within 15q11-13 were equivalently associated (Table 1 and Fig. 2A). These results suggest that specific homologous association occurs at the imprinted 15q11-13 regions.

If the imprinted region is involved in the interaction between homologs, then alterations in the normal biparental contribution of 15q11-13 would be predicted to affect the association. We therefore analyzed chromosome 15 interhomolog distances in lymphocytes from a PWS patient with two maternal copies of chromosome 15 and from an AS patient with two paternal chromosomes 15 (Fig. 3). Homologous D15Z1 distances were within the random distribution in all stages of the cell cycle in both the PWS (Fig. 3A) and AS (Fig. 3B) samples. Late S phase nuclei from these two patients exhibited different distributions of D15Z1 interhomolog distances compared to those of a normal individual (Fig. 1B). In addition, cells from patients with maternal or paternal deletion of 15q11-13 displayed no D15Z1 association in the late S phase compared to the same analysis in a second normal individual (Table 2).

We also investigated the possibility of association at a second imprinted locus. *H19* is a maternally expressed imprinted gene on human chromosome 11p15, a region that contains at least two oppositely imprinted genes (*2*). Analysis of the *H19* probe together with D15S128 (15q11-13)

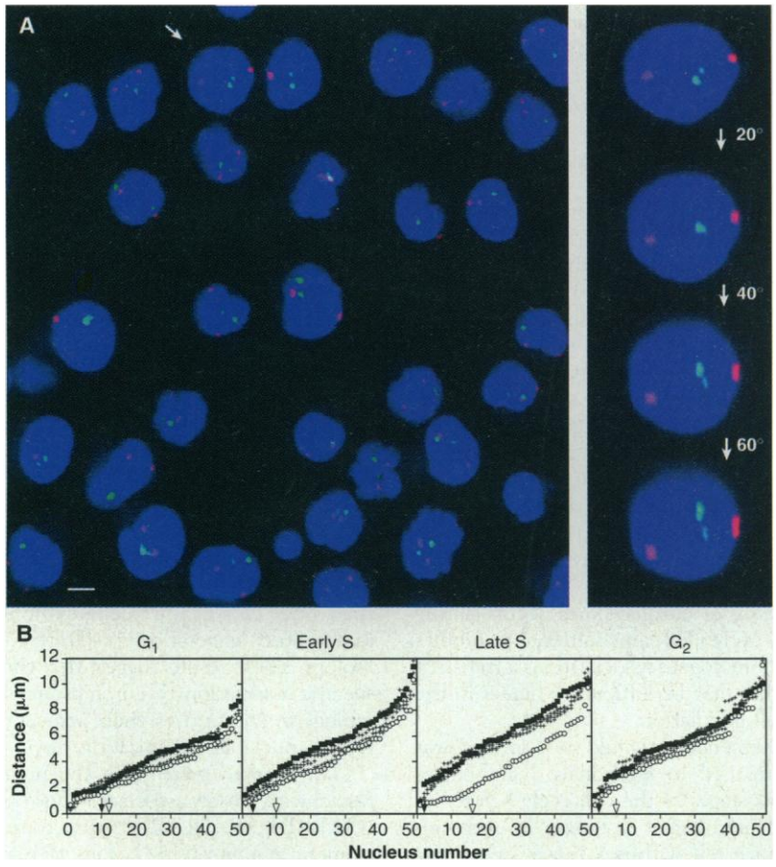

Fig. 1. Detection of chromosome 15 association in the late S phase. (**A**) A 3D look-through projection image of a field of spatially intact nuclei (total DNA pseudocolored in blue) simultaneously hybridized with a chromosome 15 centromeric probe (D15Z1, green spots) and a chromosome 12 centromeric probe (D12Z3, red spots). The scale bar represents 5 μm. Two signals are detected for each probe in each nucleus, but some require a rotation of the projection angle to distinguish two signals that lie in the same *xy* plane but have different *z* coordinates. This is demonstrated by rotation of one nucleus (indicated by the arrow) downward 20°, 40°, and 60°. For this nucleus, the two green D15Z1 signals appear to be together at 20°, but separate at other rotation angles. (**B**) Two homologous distances [green-green and red-red, 4.2 and 10.6 μm, respectively, for the nucleus in (A)] and four heterologous distances (green-red) were determined in a data set of 50 nuclei, as described previously for meiotic pairing in yeast (*22*). These six distances from each nucleus were entered in a row of six columns (two homologous distances and four randomly distributed heterologous distances), each column was independently sorted in ascending order, and each new row was given an ascending but arbitrary nucleus number (*x* axis). To enrich cell cycle stages, before 3D FISH analysis we sorted normal lymphocytes into the following phases: G_1, early S, late S, and G_2 (*9*). Heterologous distances (+) are random and form the linear swarm expected for a random distribution. D12Z3 homologous distances (closed squares) fall within this random distribution in all fractions, whereas D15Z1 (open circles) distances fall below the linear curve only in the late S phase. Arrows point to the number of nuclei with interhomolog distances ≤2.0 μm for D15Z1 (open arrows) and D12Z3 (closed arrows). With the use of a *t* test based on range, the number of nuclei with D15Z1 interhomolog distances ≤2.0 μm was significantly outside the heterologous range within 99% confidence levels ($P < 0.01$) for the G_1, early S, and G_2 fractions, but within 99.9% confidence levels ($P < 0.001$) for the late S phase fractions. A similar result was obtained in experiments with cell cycle–fractionated B lymphoblasts transformed by human Epstein-Barr virus (*10*).

Table 2. Analysis of chromosome 15 association in PWS and AS patients with 15q11-13 deletions. Late S phase lymphocytes from a second normal individual, a PWS patient with a paternal deletion of the entire 15q11-13 region (*8*), and an AS patient with maternal deletion of 15q11-13 were analyzed in duplicate experiments (Exp. 1 and Exp. 2) for D15Z1 and D12Z3 distances. The number of nuclei with interprobe distances ≤2.0 μm was extracted from the graphical analysis of 50 nuclei and is compared to the random range of heterologous distances for significance. To ensure the sensitivity and reproducibility of this analysis, each experiment was repeated and a mixing experiment was performed with the use of nuclei from normal individuals and patients in a 1:1 ratio. Slides (including Exp. 2 samples) were coded and analyzed in a blinded fashion to ensure a lack of investigator bias in results. The number of nuclei with D15Z1 interhomolog distances ≤2.0 μm in the mixed samples was about half the difference between those of normal individuals (av. normal) and those of patients (av. paternal del. or av. maternal del.) such that {[(av. normal − av. pat. del.)/2] + av. pat. del., 13.5 expected, 13 observed; [(av. normal − av. mat. del.)/2] + av. mat. del., 14 expected , 15 observed}.

Sample	Number of nuclei with interprobe distances ≤2.0 μm		
	D15Z1 probe	D12Z3 probe	Heterologous probes (mean ± range)
Normal (Exp. 1)	19*	4	4.5 ± 3
Normal (Exp. 2)	20*	4	8.5 ± 2.5
Pat. del. (Exp. 1)	8	6	6.5 ± 3
Pat. del. (Exp. 2)	7	3	5 ± 2.5
Mat. del. (Exp. 1)	9	4	4 ± 2.5
Mat. del. (Exp. 2)	8	8	7.25 ± 3
Normal + pat. del.	13	1	2.5 ± 3.5
Normal + mat. del.	15*	1	3.5 ± 2

*$P < 0.002$ by the *t* test.

revealed that interhomolog distances at both loci were significantly less than heterologous distances in the late S phase (*10*). Thus, nonrandom association of homologs may occur at other imprinted loci in addition to chromosome 15q11-13.

We have shown that a preferential association occurs between chromosome 15 homologs at the q11-q13 region in normal human lymphocytes. Previous evidence for homologous association in mammalian cells has generally been contradictory (*16*), with most 3D studies showing a random distribution of homologous chromosomes (*12, 17*). Consistent with previous work (*12*), we observed no significant interhomolog association of chromosome 12 in any phase of the cell cycle. Our observations that the homologous association was closest at the imprinted 15q11-13 region, that a biparental contribution of 15q11-13 was required, and that homologous association occurs at a second imprinted locus strongly suggest a role for parental imprinting in the preferential association of chromosome 15 homologs.

Imprinted genes appear to be clustered in chromosomal domains that show allele-specific differences in transcription, replication timing, and methylation (*1–3*), which can be coordinately regulated by cis-acting enhancers or "imprinting centers" (*18, 19*). Our results imply that transacting elements may also be involved in the regulation of imprinting as suggested (*6, 20*). Allele-specific differences in transcription, methylation, and replication may mediate or facilitate trans interactions between imprinted domains. Uniparental inheritance, hemizygous deletion, or mutation of imprinted 15q11-13 domains could not only alter normal imprinting in 15q11-13 (resulting in PWS or AS), but could also disrupt association.

The homologous association occurs only in the late S phase, which suggests a temporal as well as a spatial control of parental imprinting. Even in fractionated late S phase lymphocytes (progression time, ~3 hours), close associations are not observed in all cells, which suggests an interaction of limited duration. The instability of multiple interstitial interactions may also explain the incomplete interhomolog association, consistent with a "kissing model" of chromosome pairing previously proposed for pairing in yeast (*8*). Trans sensing of oppositely imprinted domains at a specific stage of the cell cycle may thus be crucial for the maintenance of allele-specific DNA methylation and transcription during somatic cell divisions.

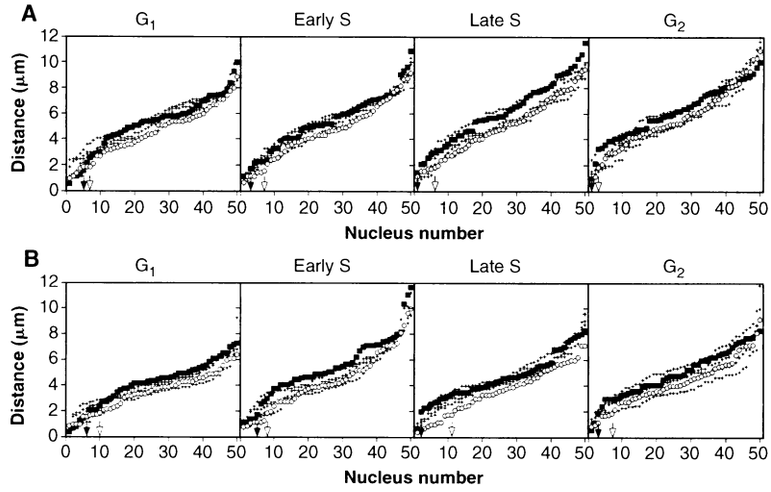

Fig. 3. Determination of chromosome 15 interhomolog distances in PWS and AS patients lacking a biparental contribution to 15q11-13. (**A**) The analysis of D15Z1 and D12Z3 in fractionated lymphocytes from a PWS patient with maternal chromosome 15 disomy (*23*) was performed as described in Fig. 1B. A random distribution of D15Z1 homologous distances is observed in all cell cycle stages. Significance was determined as in Fig. 1B: G_1 and early S, $P < 0.01$; late S and G_2, not significant. (**B**) Fractionated lymphocytes from an AS patient with paternal disomy of chromosome 15 (*24*) also exhibit a random distribution of homologous D15Z1 distances, unlike that of normal individuals. Late S, $P < 0.01$; G_1, early S, and G_2, P is not significant. In data not shown, no significant difference was found between the number of nuclei exhibiting interhomolog distances ≤2.0 μm in the late S phase nuclei from a paternal disomy at either acrocentric locus GABRB3/A5 or D13S104 (6% and 8%, respectively, 5 ± 3% random range).

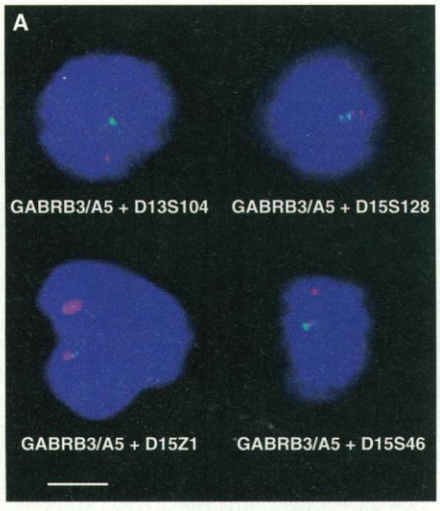

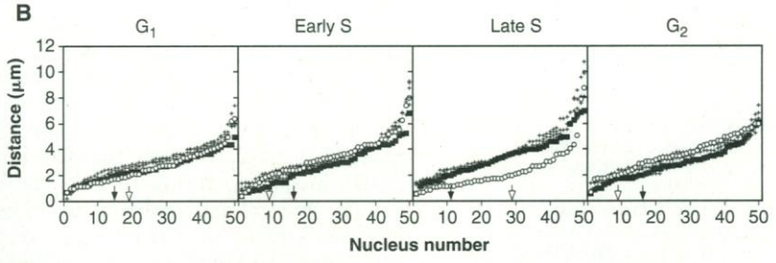

Fig. 2. Detection of chromosome 15 association with region-specific probes. (**A**) Representative projection images of late S phase nuclei hybridized with region-specific probes, demonstrating association of 15q11-13. A P1 phage specific for the region between GABRB3 and GABRA5 (green signal in all images) was hybridized with other probes (red signal) as labeled. Projection images were rotated to best visualize the separation of paired signals. The scale bar represents 5 μm. GABRB3/A5 has a closer interhomolog distance than D13S104 (a pericentromeric probe from acrocentric chromosome 13, red signal). Representative images also show that GABRB3/A5 and D15S128 have equivalent association, GABRB3/A5 is closer than D15Z1, and GABRB3/A5 is closer than D15S46 (Table 1). (**B**) Data from flow-sorted lymphocytes in which the interhomolog distances of GABRB3/A5 (open circles) are less than those of D13S104 (closed squares) and of the heterologous distances (+) only in the late S phase. Arrows point to the number of nuclei with interhomolog distances ≤2.0 μm for GABRB3/A5 (open arrows) or D13S104 (closed arrows). GABRB3/A5 interhomolog distances ≤2.0 μm were significantly outside the acrocentric heterologous range only in the late S phase ($P < 0.001$), whereas D13S104 interhomolog distances were not significantly different than the heterologous range. In data not shown, a probe from D15S128 also demonstrated more frequent interhomolog distances ≤2.0 μm than D13S104 (54% compared to 20%, 28 ± 8% random range), whereas a nonimprinted chromosome 15 control probe (D15S46) did not demonstrate significant association compared to D13S104 (38% compared to 22%, 30 ± 14% random range) in the late S phase fraction.

REFERENCES AND NOTES

1. H. V. Crouse, *Genetics* **45**, 1429 (1960); A. Razin and H. Cedar, *Cell* **77**, 473 (1994).
2. S. Zemel, M. S. Bartolomei, S. M. Tilghman, *Nature Genet.* **2**, 61 (1992).
3. D. Kitsberg *et al.*, *Nature* **364**, 459 (1993).
4. M. Lalande, *Nature Genet.* **8**, 5 (1994); R. D. Nicholls, J. H. M. Knoll, M. G. Butler, S. Karam, M. Lalande, *Nature* **342**, 281 (1989); S. Malcolm *et al.*, *Lancet* **337**, 694 (1991).
5. J. H. M. Knoll, S.-D. Cheng, M. Lalande, *Nature Genet.* **6**, 41 (1994).
6. J. M. LaSalle and M. Lalande, *ibid.* **9**, 386 (1995).
7. Y. Hiraoka *et al.*, *J. Cell Biol.* **120**, 591 (1993); B. Judd, *Cell* **53**, 841 (1988); V. Pirrotta, *BioEssays* **12**, 409 (1990); K. D. Tartof and S. Henikoff, *Cell* **65**, 201 (1991).
8. N. Kleckner and B. M. Weiner, *Cold Spring Harbor Symp. Quant. Biol.* **58**, 553 (1993).
9. Human T lymphocytes were isolated and flow-sorted on the basis of DNA content as described previously, except "early S" includes the S_1 and S_2 fractions, whereas "late S" includes the S_3 and S_4 fractions (*6*). A modified FISH protocol was developed that minimizes alterations in the normal spatial organization of the nucleus (*21*). Cells were adhered for 5 min to poly-D-lysine–coated slides, fixed 15 min in 4% paraformaldehyde and 1% methanol in phosphate-buffered saline (PBS), washed twice in 0.3 M glycine and PBS, permeabilized for 10 min in 0.5% Tween and 0.2 N HCl, washed twice in 2× saline sodium citrate (SSC), denatured 3 min in 70% formamide and 2× SSC, washed twice in 0.5% Tween and PBS and twice in 2× SSC at 4°C, then hybridized and washed as previously described (*6*) without detection steps. D15Z1 (pHSR) and D12Z3 (pA12H8, ATCC) were directly labeled by nick translation with Cy3- and Cy5-labeled deoxycytidine triphosphate (Biological Detection), respectively, and nuclei were counterstained with YOPRO (Molecular Probes). Nuclei were imaged by a Molecular Dynamics CLSM Multiprobe 2001 with an Ar/Kr laser. Imagespace software (Molecular Dynamics) was used for scanning, analysis, and projection images. Nuclei were densely distributed (Fig. 1A), and we selected clusters of 6 to 20 nuclei by using only the DNA counterstain filter to avoid bias in selection. Optical sections were scanned with a 60× objective at a 0.21, 0.21, 0.29 voxel resolution and a total image size of 512 by 512 pixels. Hybridization efficiency was 85% (number of nuclei with two red and two green signals out of the total number of nuclei scanned, in an average of four representative experiments). The *x*, *y*, and *z* coordinates were defined at the center of each hybridization signal and used to measure 3D distance by a mouse-driven cursor.
10. J. M. LaSalle and M. Lalande, unpublished results.
11. P. Emmerich *et al.*, *Exp. Cell Res.* **181**, 126 (1989); J. P. Lewis, H. J. Tanke, A. K. Raap, G. C. Beverstock, H. Kluin-Nelemans, *Hum. Genet.* **92**, 577 (1993); L. Manuelidis, *Science* **250**, 1533 (1990).
12. M. Ferguson and D. C. Ward, *Chromosoma* **101**, 557 (1992).
13. Mean nuclear diameter was 8 μm with a range of 6 to 12 μm, as determined by the 3D object count feature of Imagespace software. No substantial differences in nuclear diameter were observed between different cell cycle fractions.
14. The distance of 2.0 μm was chosen on the basis of a comparison of the graph of late S phase lymphocytes to that of premeiotic yeast (*22*). The degree of nonrandomness was similar, but the scale of the graphs was different because the diameter of yeast nuclei was ~5 μm, whereas lymphocytes are ~6 to 12 μm (*13*). Pairing in premeiosis and meiosis may involve a tighter association between homologs, or yeast chromosomes may have fewer spatial constraints than chromosomes in higher eukaryotes, thus explaining the difference in actual distances.
15. Single-copy probes were labeled with biotin or digoxigenin and detected with anti-digoxigenin-fluorescein (green) and Cy3-avidin (red) as previously described (*9*), but with 0.5% Tween in the last wash. To increase cell density, we fixed and washed the cells in suspension, then cytocentrifuged them at 55*g* for 4 min before permeabilization. There was no detectable change in nuclear shape by a *z* scan. Hybridization efficiencies were 75%. Separation of sister chromatid FISH signals at replicated sites was observed infrequently as a result of the low resolution of pixel aquisition (0.21 μm^2), lack of physical spreading of DNA by the altered FISH protocol, and larger probe size (centromeric repeats and 80- to 120-kb P1 clones). In the infrequent cases where replication doublets were observed, the measurement was taken at the point between the two signals. Source numbers for P1 clones at Genomesystems are as follows: GABRB3/A5, 2269; D15S113, 6343; D13S104, 6269; D15S128, 7207; and D15S46 (ATCC).
16. T. Haaf and M. Schmid, *Exp. Cell Res.* **192**, 325 (1991).
17. S. A. Lesko, D. E. Callahan, M. E. LaVilla, Z.-P. Wang, P. O. P. Ts'o, *ibid.* **219**, 499 (1995); L. Manuelidis, *Hum. Genet.* **71**, 288 (1985).
18. P. A. Leighton, J. R. Saam, R. S. Ingram, C. L. Stewart, S. M. Tilghman, *Genes Dev.* **9**, 2079 (1995); P. A. Leighton, R. S. Ingram, J. Eggenschwiler, A. Efstratiadis, S. M. Tilghman, *Nature* **375**, 34 (1995); J. S. Sutcliffe *et al.*, *Nature Genet.* **8**, 52 (1994); K. Buiting *et al.*, *ibid.* **9**, 395 (1995).
19. P. H. Gunaratne, M. Nakao, D. H. Ledbetter, J. S. Sutcliffe, A. C. Chinault, *Genes Dev.* **9**, 808 (1995).
20. J.-Y. Tsai and L. M. Silver, *Genetics* **129**, 1159 (1991).
21. R. T. O'Keefe, S. C. Henderson, D. L. Spector, *J. Cell Biol.* **116**, 1095 (1992).
22. B. M. Weiner and N. Kleckner, *Cell* **77**, 977 (1994).
23. Patient G1478 in W. P. Robinson *et al.*, *Eur. J. Hum. Genet.* **1**, 280 (1993).
24. Patient AS136 in A. Bottani *et al.*, *Am. J. Med. Genet.* **51**, 35 (1994).

25. We thank W. Robinson, K. Hirschorn, S. Orkin, A. Bottani, B. Horsthemke, R. Wharton, J. Holden, B. White, M. Higgins, A. Flint, K. Glatt, Q. M. Liu, H. Lidov, J. Wagstaff, and L. M. Kunkel for their help and important contributions to this work. Supported by Howard Hughes Medical Institute and NIH grant RO1-NS30628.

7 December 1995; accepted 6 March 1996

Amelioration of Vascular Dysfunctions in Diabetic Rats by an Oral PKC β Inhibitor

Hidehiro Ishii, Michael R. Jirousek, Daisuke Koya, Chikako Takagi, Pu Xia, Allen Clermont, Sven-Erik Bursell, Timothy S. Kern, Lawrence M. Ballas, William F. Heath, Lawrence E. Stramm, Edward P. Feener, George L. King*

The vascular complications of diabetes mellitus have been correlated with enhanced activation of protein kinase C (PKC). LY333531, a specific inhibitor of the β isoform of PKC, was synthesized and was shown to be a competitive reversible inhibitor of PKC β_1 and β_2, with a half-maximal inhibitory constant of ~5 nM; this value was one-fiftieth of that for other PKC isoenzymes and one-thousandth of that for non-PKC kinases. When administered orally, LY333531 ameliorated the glomerular filtration rate, albumin excretion rate, and retinal circulation in diabetic rats in a dose-responsive manner, in parallel with its inhibition of PKC activities.

The major causal factor in the development of retinopathy and nephropathy in diabetes mellitus is hyperglycemia (*1*). One theory (*2*) has attributed the adverse effect of hyperglycemia to the activation of PKC, a family of serine-threonine kinases that regulate many vascular functions, including contractility, hemodynamics, and cellular proliferation (*3*, *4*). PKC activity is increased in the retina, aorta, heart, and renal glomeruli of diabetic animals, probably because of an increase in de novo synthesis of diacylglycerol (DAG), a major endogenous activator of PKC (*2*, *5*, *6*). Our observation that the PKC β_2 isoenzyme is preferentially activated in the retina, heart, and aorta of diabetic rats (*2*) led us to propose that the abnormal activation of PKC β_2 may cause some of the diabetic vascular complications (*5*). To test this hypothesis, we synthesized an orally effective PKC inhibitor that was PKC β selective and evaluated its ability to ameliorate vascular dysfunctions in diabetic rats.

On the basis of the structures of known PKC inhibitors (*7*, *8*), we performed an extensive screening to identify and optimize a PKC β–selective inhibitor. A panel of eight cloned human PKC isoenzymes (α, β_1, β_2, γ, δ, ε, ζ, and η) was used to profile the selectivity of the inhibitor, with DAG used as an activator (*3*, *8*). The macrocyclic bis(indolyl)maleimide structure (LY333531) was found to inhibit PKC β selectively (Scheme 1). LY333531 inhibited PKC β_1 and β_2 with a half-maximal inhibitory constant (IC_{50}) of 4.7 and 5.9 nM, respectively, whereas for other PKC isoenzymes except η, the IC_{50} was 250

H. Ishii, D. Koya, C. Takagi, P. Xia, A. Clermont, S.-E. Bursell, E. P. Feener, G. L. King, Research Division, Joslin Diabetes Center, Department of Medicine, Brigham and Women's Hospital and Harvard Medical School, 1 Joslin Place, Boston, MA 02215, USA.
M. R. Jirousek, W. F. Heath, L. E. Stramm, Lilly Laboratories, Indianapolis, IN 46285, USA.
T. S. Kern, Department of Ophthalmology, University of Wisconsin, Madison, WI 53706, USA.
L. M. Ballas, Sphinx Pharmaceutical, Durham, NC 27707, USA.
*To whom correspondence should be addressed.